World Journal of Engineering Research and Technology
WJERT
www.wjert.org
SJIF Impact Factor: 5.218

BRUSHLESS SLIP POWER RECOVERY VERSION OF A HOMOPOLAR INDUCTOR MACHINE

Dr. Elhussien A. Mahmoud*

Article Received on 21/03/2018 **Article Revised on 11/04/2018** **Article Accepted on 01/05/2018**

***Corresponding Author**
Dr. Elhussien A. Mahmoud

ABSTRACT

The aim of this paper is to present a novel design for the homopolar inductor machine which allows changing the armature frequency using the field circuit frequency at constant rotor speed. Or in other words, The proposed machine is able to provide armature voltage of constant frequency while coupled to a variable speed prime mover. The armature winding is directly connected to the grid without back to back inverter. The elimination of the armature circuit power electronics reduces the overall cost. In brief, the proposed machine has two field windings which are supplied by two phase alternating current. A rotating field is established with an angular speed proportional to the field supply frequency relative to the rotor body. When the rotor revolves, the rotor pulls the flux lines in the same direction of the rotor rotation. The flux speed relative to the stationary armature winding is the resultant of the field supply angular speed and the rotor speed in electrical angle. As the rotor speed changes, it is possible to change the field supply frequency for compensation and keep the armature output frequency constant. In motoring mode, with constant armature voltage magnitude and frequency, the field supply frequency is able to regulate the rotor speed.

KEYWORDS: Homopolar, slip power recovery, homo-hetropolar, inductor machine, wind energy, traction.

INTRODUCTION

The homopolar inductor alternator (HIA) has the superiority on the classical synchronous machine in eliminating the rotor winding. The elimination of the rotor windings increases the overall machine robustness and reliability.[1,2] The location of the field winding on the rotor of the classical synchronous machine results in the need of slip rings or an additional exciter

alternator and rotating rectifier. The mechanical strength of the field winding is a barrier which limits the classical synchronous machine mechanical speed. Alternatives to HIA design are the reactive homopolar brushless synchronous machine (RHBSM) and the reactive homo-hetropolar brushless synchronous machine (RHHBSM).[3,4] The rotor construction of the RHBSM is simpler than that of the RHHBSM. On the other hand, the armature winding of the RHBSM is so much complicated while the RHHBSM utilizes the standard winding configurations.

Electrical power generation based on wind turbines suffers from the fact of variable wind speed and variable alternator rotor speed in consequence. The grid connected wind farm requires a full rating back to back converter to adapt the generated power to the grid frequency while using the classical synchronous alternator. Similarly, the plain induction machine needs the full rated power electronics to control the machine torque and slip. The utilization of the category of the slip power recovery machines reduces the power electronics rating to third or even a quarter of the total power delivered. An example is the doubly fed induction generator (DFIG) which has the drawback of using slip rings.[5] Alternatively, the brushless doubly fed induction generator (BDFIG) takes over with the disadvantage of complicated rotor cage structure and rotor losses.[6] The brushless doubly fed reluctance generator (BDFRG) overcome the rotor losses problem but with poor dynamic performance.[7] This paper provides an alternative slip power recovery machines. First, the paper introduces the cascade connection of two HIA, RHBSM or RHHBSM to provide constant armature voltage frequency at variable rotor speed. Then a novel design of the HIA which simulate the two machine cascade connection is introduced. The proposed machine is named the brushless slip recovery homopolar machine (BSRHM).

II- Voltage Equation of the Cascaded Synchronous Homopolar Machines

In the homopolar arrangement, the flux lines approach the rotor through the axial direction then the flux is distributed among the rotor salient poles in the radial direction. The direction of the entire flux lines is unique either from the rotor centre towards the rotor perimeter or in the opposite direction. The whole flux is assumed occupying the salient poles while the minor flux in the inter pole area is neglected. All the real salient poles have the same magnetic polarity. Supposing there are a number of imaginary poles occupying the inter-pole regions and having the opposite magnetic polarity, a sinusoidal flux distribution along the air gap can be assumed with a number of pole pair (P) equal to the rotor real poles. As the imaginary

poles do not provide any flux, the flux density is assumed to be a half wave rectified cosine wave coincident with the real pole axes.

Figure (1) demonstrates two identical homopolar synchronous machines coupled together on the same shaft with special angular phase shift. The shown configuration is for two real poles. Four arbitrary conductors shifted by complete pole pitch are shown and are denoted by T, R, B and L for the top, right, bottom and left mechanical positions respectively.

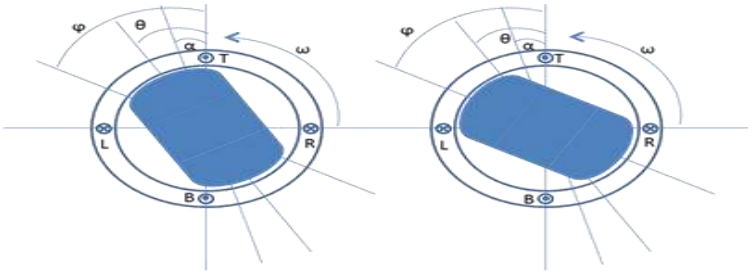

Figure 1: Two four poles cascaded synchronous homopolar machines.

Considering the left side machine, on the assumption of DC field excitation and based on equation (1), the EMF in the T and B conductors is equal to the maximum value if the rotor angle θ equal to zero.

$$EMF = \beta l V \qquad (1)$$

Where

β is the air gap flux density.

l is the conductor length.

V is the air gap flux peripheral speed

The possible connection from T to B conductors leads to subtraction of the EMF of both conductors and zero resultant voltage in consequence. As the other two conductors L and R lie under the imaginary poles and have zero induced voltage, the correct connection is T L B R or T R B L. When the rotor angle is π/2 mechanical degree, the EMF induced in the L and R conductor is maximum, while that in T and B will be zero. But due to the connection sequence of the conductors, it will be negative of the maximum value. The expected resultant EMF waveform is sinusoidal with frequency double that of the rotor mechanical rotation. In general the EMF frequency is the number of rotor real poles multiplied by the rotor mechanical frequency.

To analyze the case of alternating field excitation, it is required to calculate the flux linkage in the stator winding due to the rotor excitation. The conductors T and L are seen as a coil. Conductors L and B also forming a coil but it is place opposite to the T-L coil. Assuming the flux lines are passing from the rotor centre to the rotor perimeter and are seen by T-L and B-R coils as positive flux linkage. Then the flux is seen by L-B and R-T coils as negative flux linkage. Equation (2) describes the flux density of the left side machine.

$$\beta(\theta) = \begin{cases} \beta_m \cos(P\theta) \ \forall \ \dfrac{-\pi}{2P} < \left(\theta \pm \dfrac{2m\pi}{P}\right) < \dfrac{\pi}{2P} \\ zero \quad \forall \ \dfrac{\pi}{2P} < \left(\theta \pm \dfrac{2m\pi}{P}\right) < \dfrac{3\pi}{2P} \\ m \text{ is positive integer} \end{cases} \tag{2}$$

Assuming an arbitrary angle α, the flux linking the stator winding (λ) is given by equation (3)

$$\lambda = T_{ph} \int_0^{2\pi} \beta(\theta - \alpha) lr d\alpha \tag{3}$$

Where

r is the rotor radius.

Substituting from equation (2) into equation (3) resulting in equation (4). Then the flux linkage of the left side machine in got by integrating equation (4) as in equation (5)

$$\lambda_l = T_{ph} lr\beta_m \left\{ \int_0^{\frac{\pi}{2P}+\theta} \cos(P(\theta - \alpha)) d\alpha - \int_{-\frac{\pi}{2P}+\theta}^{0} \cos(P(\theta - \alpha)) d\alpha \right\} \tag{4}$$

$$\lambda_l = 2T_{ph} lr\beta_m \sin(P\theta) \tag{5}$$

Where: the subscript *l* refers to the left side machine.

Similarly, the equation of the right side machine is given by equation (6)

$$\lambda_r = T_{ph} lr\beta_m \left\{ \int_0^{\frac{\pi}{2P}+\emptyset} \cos(P(\emptyset - \alpha)) d\alpha - \int_{-\frac{\pi}{2P}+\emptyset}^{0} \cos(P(\emptyset - \alpha)) d\alpha \right\}$$
$$= 2T_{ph} lr\beta_m \sin(P\emptyset) \tag{6}$$

Where: the subscript *r* refers to the right side machine.

Both machines are excitation with sinusoidal current of the same amplitude and frequency while a π/2 phase angle is maintained between them. Moreover, the spatial angular shift between the hubs of the two machines is governed by equation (7).

$$\emptyset = \theta + \frac{\pi}{2P} \tag{7}$$

On the assumption of linear magnetic circuit, equation (5 and 6) can be rewritten as in equation (8 and 9)

$$\lambda_l = KI_{fm} \sin(\omega_f t + \delta) \sin(P\theta) \tag{8}$$

$$\lambda_r = KI_{fm} \sin(\omega_f t + \frac{\pi}{2} + \delta) \sin(P\theta + \frac{\pi}{2}) \tag{9}$$

Where: K is a proportionality factor.

δ is the field current phase angle.

I_{fm} is the field current amplitude.

ω_f is the field current angular velocity.

The induced EMF in both machines can be found using the well Known voltage equation given by equation (10).

$$EMF = \frac{d\lambda}{dt} + \frac{d\lambda}{d\theta} \times \frac{d\theta}{dt} \tag{10}$$

The EMF induced in the left and right side machines are given in equation (11 and 12) respectively. Where the factor K and I_{fm} are dropped from the equation to simplify the analysis.

$$EMF_l = \omega_f \cos(\omega_f t + \delta) \sin(P\theta) + \omega_r P\cos(P\theta) \sin(\omega_f t + \delta) \tag{11}$$

$$\begin{aligned} EMF_r &= \omega_f \cos(\omega_f t + \frac{\pi}{2} + \delta) \sin(P\theta + \frac{\pi}{2}) + \omega_r P\cos(P\theta + \frac{\pi}{2}) \sin(\omega_f t + \frac{\pi}{2} + \delta) \\ &= -\omega_f \cos(P\theta) \sin(\omega_f t + \delta) - \omega_r P\cos(\omega_f t + \delta) \sin(P\theta) \end{aligned} \tag{12}$$

Where

$$\omega_r = \frac{d\theta}{dt} \tag{13}$$

The main idea of the cascade connection of two synchronous homopolar machines is summarized in the following conditions

1- The two machines are identical.
2- The two machines are coupled together with the stator frames are fully aligned while the rotor position is specially shifted according to equation (7)
3- The field windings in the two machines are supplied by a two phase current; each phase supply only one of the two machines field coil.
4- The two machines armature winding are connected in series such that the output voltage are added together.

The resultant EMF of the cascade connection is given by equation (14) and is rearranged through equations (15-18)

$$EMF = EMF_r + EMF_l \quad (14)$$

$$EMF = (\omega_f - P\omega_r)\left[\cos(\omega_f t + \delta)\sin(P\theta) - \cos(P\theta)\sin(\omega_f t + \delta)\right] \quad (15)$$

$$EMF = -(P\omega_r - \omega_f)\ \sin(P\theta - \omega_f t - \delta) \quad (16)$$

Equation (17) gives the integration of equation (13) based on a constant rotor speed assumption.

$$\theta = \omega_r t \quad (17)$$

Finally substituting equation (17) into equation (16) resulting in equation (18)

$$EMF = -(P\omega_r - \omega_f)\ \sin((P\omega_r - \omega_f)t - \delta) \quad (18)$$

From equation (18) it is obvious that the frequency of the armature winding EMF of the proposed cascaded system depends on both of the rotor speed and field frequency. While the frequency of the armature winding EMF in the conventional homopolar synchronous machine depends only on the rotor speed.

The final form of the induced EMF of the cascaded system is given by equation (19, 20 and 21).

$$EMF = -Z\, I_f\, f\, \sin(2\pi f t - \delta) \quad (19)$$

$$f = \frac{\omega_a}{2\pi} \tag{20}$$

$$\omega_a = \pm(P\omega_r - \omega_f) \tag{21}$$

Where Z is constant

ω_a : is the armature winding angular speed

f : is the armature frequency

I_f : is the RMS field current

III- Brushless Slip Recovery Homopolar Machine

The cascaded system proposed in the previous section is similar to the idea of the slip recovery machines, namely, the DFIG, BDFIG and BDFRG, where the primary winding frequency can be kept constant regardless of the variation of the rotor speed by adjusting the secondary winding frequency. The same principle is valid for the cascaded system. According to equation (21), it is possible to vary the field winding frequency to compensate the rotor speed effect on the armature voltage frequency.

It is possible to combine the cascaded system in a single embedded machine, which is called, The BSRHM. The proposed BSRHM can be designed in several ways. Three designs are described in this work while only one design is built as a prototype. Figure (2) illustrates the first design of the proposed BSRHM. Table (1) provides description for the machine parts break down given in figure (2). Figure (3) depicts the magnetic flux paths through the machine.

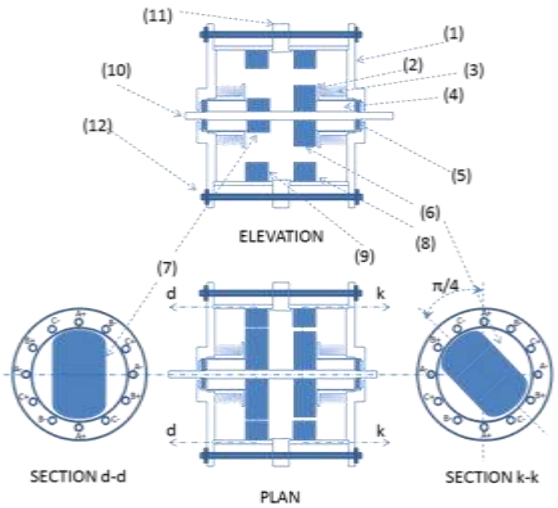

Figure 2: BSRHM design on the HIA base.

Table 1: BSRHM parts list.

Part	Description
1	End bell
2	Field coil holder
3	Field coil
4	Axial pole
5	bearings
6	Right side real poles
7	Left side real poles
8	Right side magnetic core of a dual core stator
9	Left side magnetic core of a dual core stator
10	shaft
11	Non-magnetic separator
12	Gathering bolts

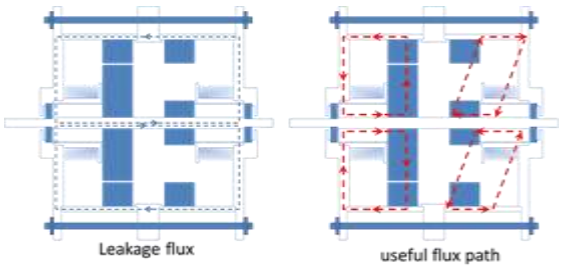

Figure 3: Flux paths in the BSRHM.

The special location of the field coils on the axial poles, shown in figure (2), force the magnetic flux to move in the paths illustrated in figure (3). The paths shown in the right side part of figure (3) contains the useful flux. The useful flux is the flux moves in the radial direction through either the left or the right real poles, armature core and cuts the armature conductors. The flux utilizes the path shown in the left side of figure (3) is considered as leakage flux and should be prevented or at least minimized. A non-magnetic material is inserted in the leakage flux path to increase the path magnetic reluctance. The proposed location of the non-magnetic material is marked by number (11) in figure (2). The gathering bolts, marked by number (12) also provide a leakage flux path. If necessary, it can be cured by a nonmagnetic slave and washers but it is negligible anyway. The angular angle required between the left and right pole sets magnetic flux can be achieved by displace the poles or the armature core. The choice of shifting the real pole axis, as shown in figure (2), simplifies the machine construction. The two stator magnetic cores are aligned in such a way that the armature conductors path in a straight line from the first core to the second core. A photo for a proper aligned dual core stator is given in figure (4). Figure (4) is actually a photo for the prototype stator which will be used in the experimental work in the next section. It is better to

fill the gap between the two cores by a third plastic core to provide mechanical support for the armature conductors.

Figure 4: BSRHM dual core stator.

There is a possibility to extend the design of both of the RHBSM and RHBSM, described in,[4] to simulate the BSRHM. Figure (5) depicts the design of a four poles BSRHM based on the RHBSM arrangement. The two phase field coils are embedded in two U shaped stator core separated by a gap or nonmagnetic material.

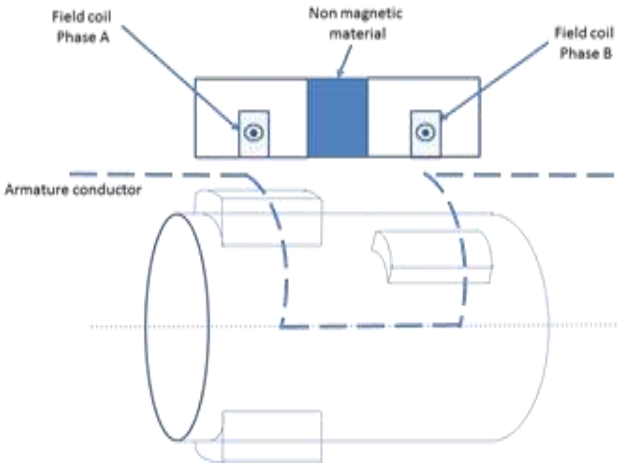

Figure 5: BSRHM design on the RHBSM base.

The armature coil takes the shape of double 8 where the conductors of each coil side changes its position (slot) twice as shown in figure (5).

Figure (6) gives the alternative design for the four poles BSRHM based on the RHHBSM. The two phase field coil is placed in two E shaped stator cores while the armature coil side passes straight in the slots between the stator laminations. The number of rotor real salient poles is doubled in the case of the RHHBSM based design.

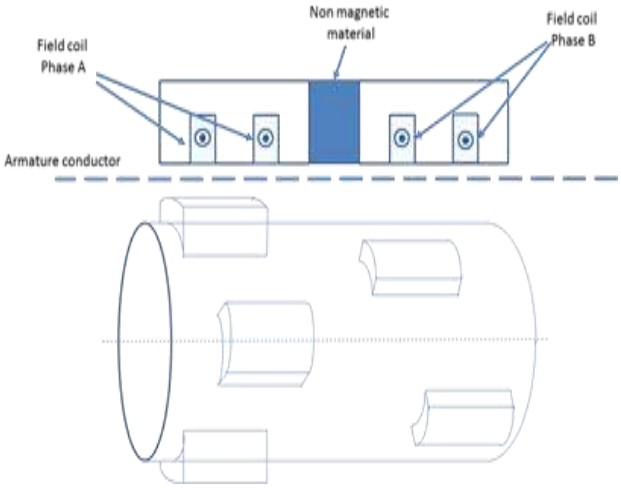

Figure 6: BSRHM design on the RHHBSM base.

IV- Muti-Phase Field and Armature Windings

The design on the RHHBSM or the RHBSM base can be extended to multiphase field windings. As the main idea is to establish a rotating field whose speed is superimposed on the rotor electrical angular speed to achieve the same frequency of the armature winding. The design based on the RHHBSM with two phase field current requires two rotor segments, each contains similar group of salient poles but shifted by $\pi/2$ electrical degree in space and two E-stator cores separated by nonmagnetic region. The n-phase field arrangement requires n rotor segments shift by $2\pi/n$ or π/n electrical degree in space and n E-stator cores. Similar approach is valid for the case of the n-phase field design based on the RHBSM. In the latter case each coil side has to change its position (slot) n-times which complicates the armature winding design. The usage of multi-phase field windings allows fault tolerant operation with one field phase open. In addition, the armature windings can be arranged in a multi-phase configuration to utilize the fault tolerance and the other multiphase machines benefits in the armature side as well. There is no relation between the number of phases in the field circuit and the number of phases in the armature circuit.

V- EPERIMANTAL RESULTS

The experimental setup shown in figure (7) is established. It consists of the proposed BSRHM, three phase induction motor (IM), Scott transformer, two shunt resistance, two VFD. The BSRHM prototype used in the experiment is four pole BSRHM built based on the HIA configuration shown in figure (2). The BSRHM is operated in the generator mode while a two poles 3 ph IM acts as a prime mover (PM) to allow operation up to double the BSRHM base speed. The prime mover speed is regulated using telemecanique VFD model Altivar 08.

The VFD output frequency is recoded from its digital screen and is used as an indication for the set up shaft speed.

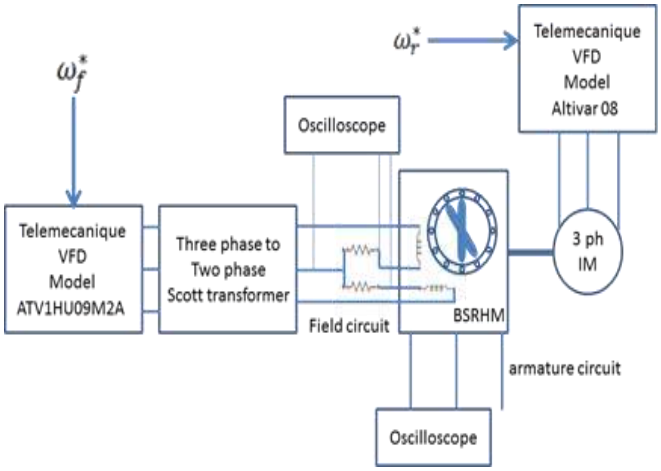

Figure 7: Block diagram of the experimental setup.

Another telemechanique VFD model ATV1HU-09M2A supplies the field coils through a three-phase to two-phase Scott transformer. Two shunt resistances are used to measure the current in both of the left and right axial pole coils. Figure (8) provide a sample of the currents flow through both of the two field coils on the same graph where the π/2 phase shift is obvious.

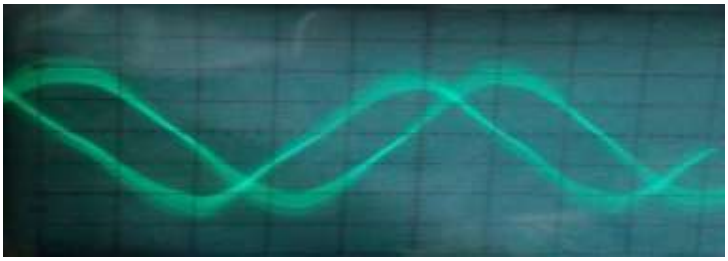

Figure 8: Two phase field current in both axial pole field coils.

The first experiment aims to verify the effect of changing the field current frequency on the armature voltage frequency at constant rotor speed. The setup runs at PM frequency of 25.5 Hz which result in 1530 RPM synchronous speed. The rotor speed is slightly less by the amount of the PM slip. At this condition, which is almost the base speed of the BSRHM, the field frequency is varied. Figure (10 A, B,...H) shows the waveform of the armature line to line voltage at field frequency of (10, 15, 20, 25, 70, 75, 80, 100) Hz respectively. From figure (9), it is shown that increasing the field frequency reduces the armature frequency until the field frequency equal the rotor electrical frequency. Then increasing the field frequency

increases the armature frequency. This statement proves the validity of equation (21). During the experiment, the armature voltage waveform was undetectable while the field frequency belongs to the region] 35, 55 [Hz. From equation (19), the amplitude of the armature voltage is proportional to the armature frequency which is null or near null at the field frequency region of] 35, 55 [Hz.

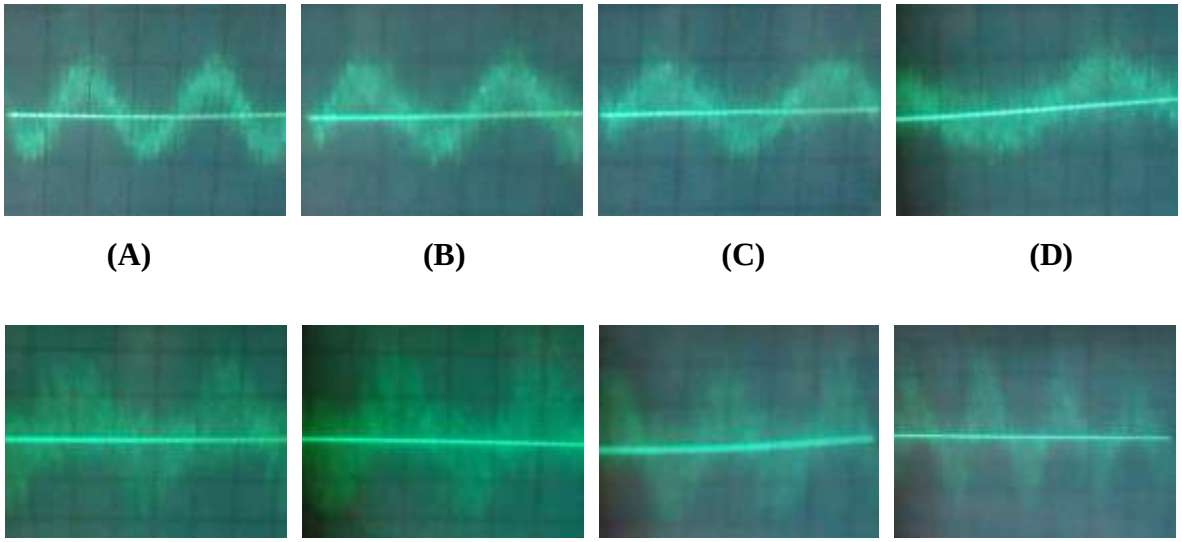

(A) **(B)** **(C)** **(D)**

(E) **(F)** **(G)** **(H)**

Figure 9: Line to line armature voltage at 25.5 Hz rotor frequency and different field frequencies.

The second experiment aims to prove the possibility of producing armature voltage of constant frequency at variable rotor speed using the field frequency as a regulation tool. The selected value of the armature voltage frequency during the experiment is 50Hz. A test signal of pure 50 Hz sine wave is measured by the oscilloscope for calibration. Then the oscilloscope leads is used to monitor the armature line to line voltage. The PM supply frequency is raised on steps. At each step the field frequency is varied until the waveform on the oscilloscope screen has the same wave length of the test signal. The field frequency is then recorded against the PM frequency. Both of the PM frequency and the field frequency are read from the inverters digital screens. The value of the field frequency that leads to 50 Hz armature frequency could be calculated by substituting in equation (21) as given in equation (22).

$$f_f = 2\, f_r - 50 \qquad (22\,a)$$

$$f_f = 2\, f_r + 50 \qquad (22\,b)$$

Where

f_r is the PM supply frequency

f_f is the calculated field frequency

The multiplication by the factor 2 is due to the difference in pole pair number between the PM and the BSRHM. Equation (22a) depicts the case of producing positive sequence armature voltage while equation (22b) represents the negative sequence case. Table (2) and table (3) shows the PM frequency, calculated field frequency and experimentally measured field frequency in Hz for the positive and negative sequence cases respectively.

Table 2: Field current frequency versus rotor speed at constant positive sequence armature frequency.

PM frequency	Experimental f_f	Calculated f_f
19.8	-18.5	10.4
23.6	-8.8	-2.8
25.5		1
30.2	6.2	10.4
34.9	15.9	19.8
39.6	25.7	29.2
45.3	36.3	40.6

Table 3: field current frequency versus rotor speed at constant positive sequence armature frequency.

PM frequency	Experimental f_f	Calculated f_f
19.8	81	89.6
23.6	90.9	97.2
25.5	94.2	101
30.2	104	110.4
34.9	115	119.8
39.6	123	129.2
45.3	135	140.6

Table (1 and 2) verify the ability of the BSRHM to produce constant frequency voltage at the armature terminals at variable rotor speed. The difference between the calculated field frequency and the experimentally measured field frequency is due to the PM slip frequency as the former is calculated based on the PM synchronous speed. The field frequency negative values are realized during the experiment by reversing the phase sequence of the 3 phase input voltage of the Scott transformer. The direction of rotor rotation is kept fixed during the whole experiment.

VI. CONCLUSION

This paper discussed the possibility of coupling a grid connected homopolar synchronous machine to variable speed wind turbine without the need of armature circuit power electronics. Cascade connection of the HIA, RHBSM or RHHBSM with a two phase field excitation is proposed to produce armature voltage with constant frequency at variable rotor speed. New machine is introduced (BSRHM) for the embedded design of the cascade connected homopolar synchronous machine. The multi-phase armature muti-phase field BSRHM is discussed. Finally, a test rig is built to validate the proposed BSRHM performance while connected to wind turbine. The experimental results prove the suitability of the BSRHM to be driven by a variable speed wind turbine while its armature is directly connected to the utility grid.

REFERENCES

1. Zhenxiu Lou, Kexun Yu, Liheng Wang, Zhang-ao Ren, and Caiyong Ye, "Two-Reaction Theory of Homopolar Inductor Alternator", IEEE TRANSACTIONS ON ENERGY CONVERSION, 2010; 25(3): 677-679.
2. Perry Tsao, Member, IEEE, Matthew Senesky, Student Member, IEEE, and Seth R. Sanders, Member, IEEE, "An Integrated Flywheel Energy Storage System With Homopolar Inductor Motor/Generator and High-Frequency Drive", IEEE transaction on industrial applications, 2003; 39(6): 1710-1725.
3. Deaconu Sorin Loan and Topor Marcel, "Torque Control of Reactive Homopolar Brushless Synchronous Machine For Traction Applications", the 18th national conference on electrical drive (CNAE), ACTA Electrotechnica, 2016; 57(3-4): 404-410.
4. Sorin Ioan Deaconu, Lucian Nicolae Tutelea, Gabriel Nicolae Popa and Tihomir Latinovici, "Mathematical models and the control of homopolar and homo-heteropolar reactive synchronous machines with stator excitation", Advances in Communications, Computers, Systems, Circuits and Devices, 2010; 78-83.
5. Mohamed Magdy, Hany M. Hasanien, Hussien F. Soliman, and Elhussien A. Mahmoud, "On-Line ANN based Controller for Improving Transient Response of Grid-Connected DFIG-Driven by wind Turbine", International Journal of Recent Trend in Engineering & Research, IJRTER, 2018; 4(4): 230-245.
6. Ramtin Sadeghi, Sayed M. Madani and Mohammad Ataei, "A New Smooth Synchronization of Brushless Doubly-Fed Induction Generator by Applying a Proposed Machine Model", IEEE Transaction on Sustainable Energy, 2018; 9(1): 371-380.

7. Elhussien A. Mahmoud, M. Nasrallah, Hussien F. Soliman and Hany M. Hasanien, "Fractional Order PI controller Based on Hill Climbing Technique for Improving MPPT of the BDF-RG Driven by Wind Turbine:, 19th international middle-east power system conference (MEPCON'19, December, 2017.